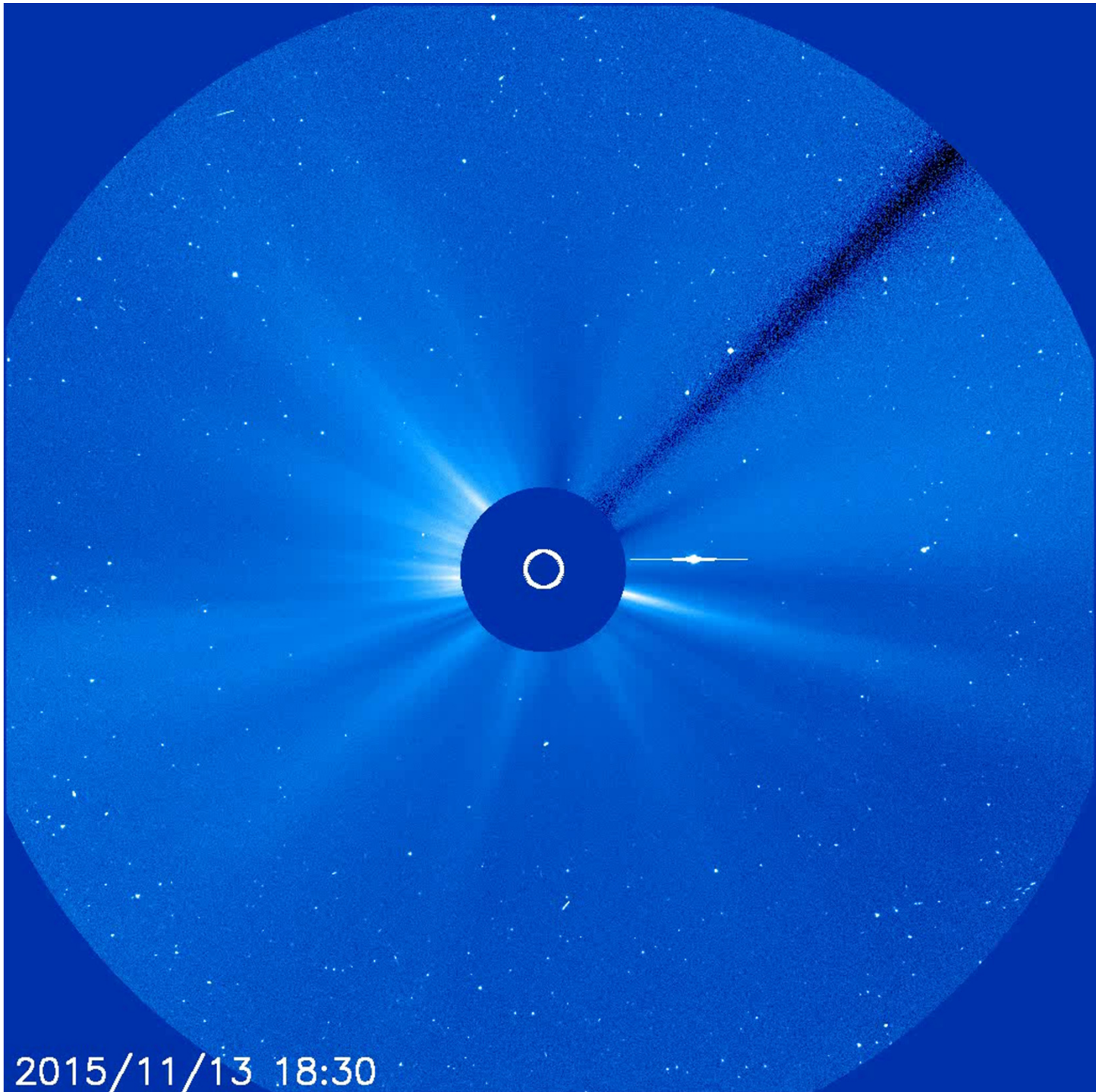


## **22. Solar Wind.**

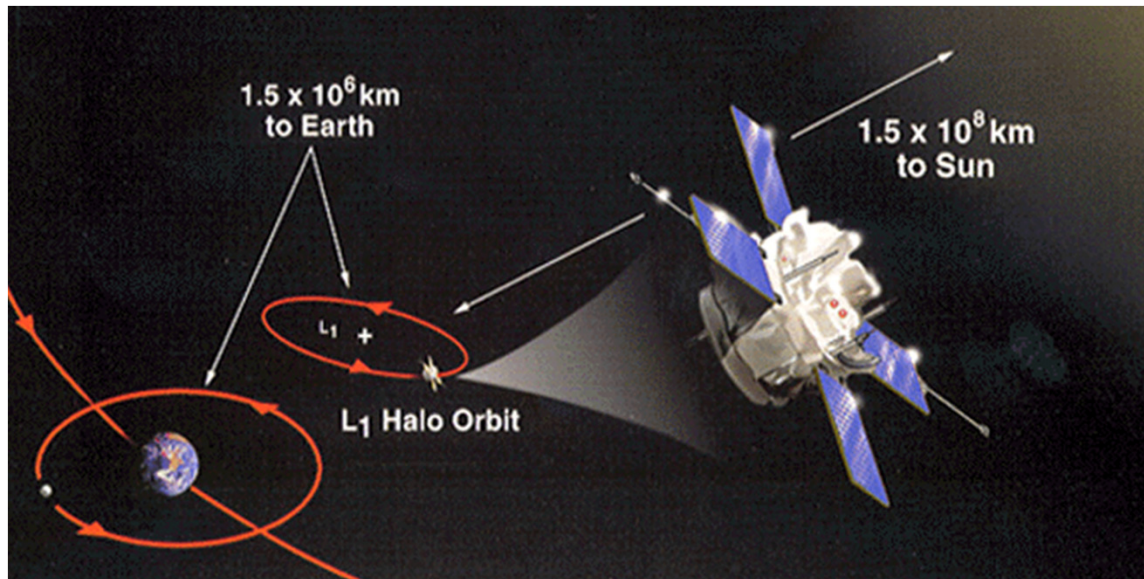
# Solar Wind

- Expansion of the Solar Corona
- Parker's solar wind model
- Magnetic Effects. Source-Surface Model.
- Interplanetary Magnetic Field (IMF)



2015/11/13 18:30

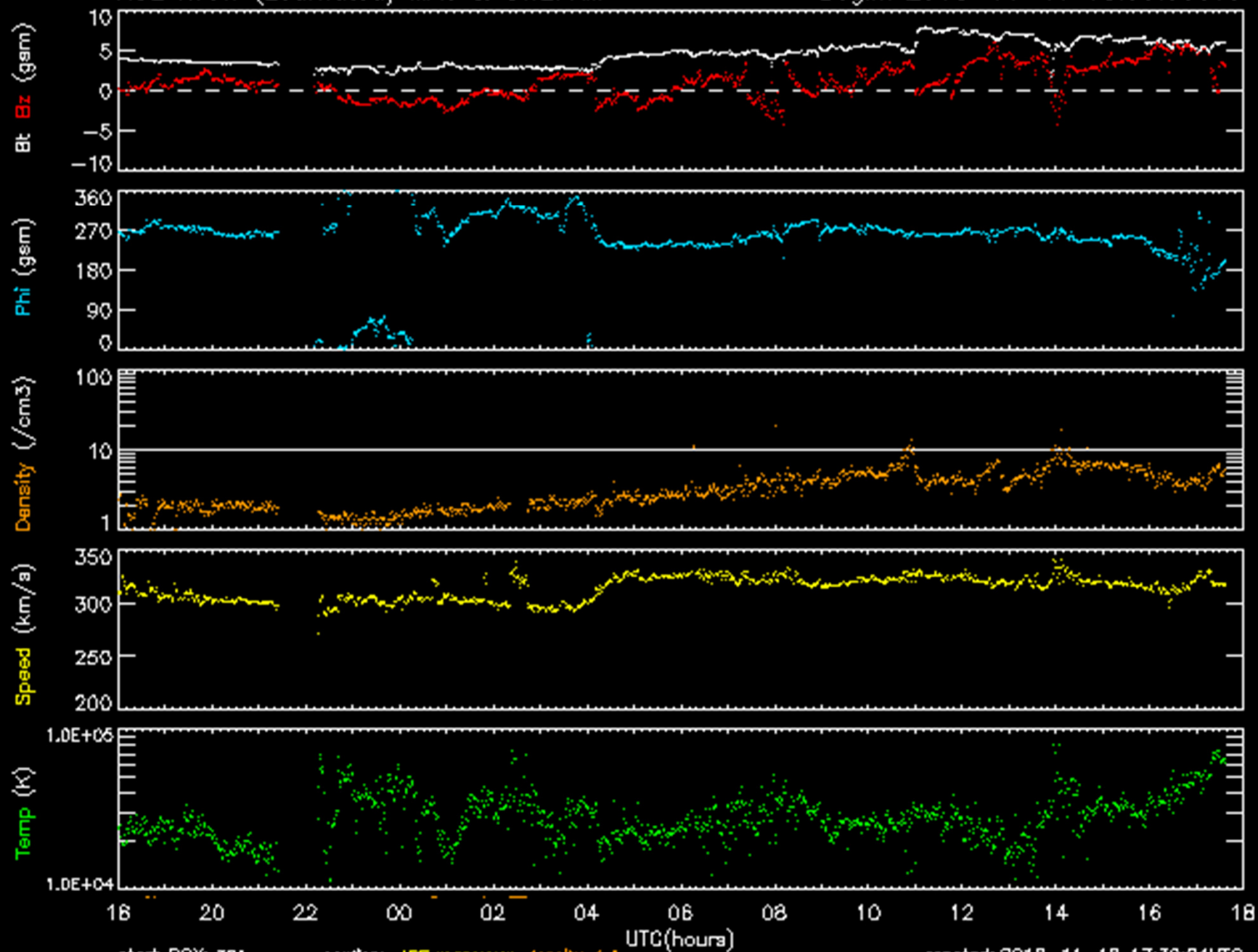
# ACE – Advanced Composition Explorer Explorer (1997-current)



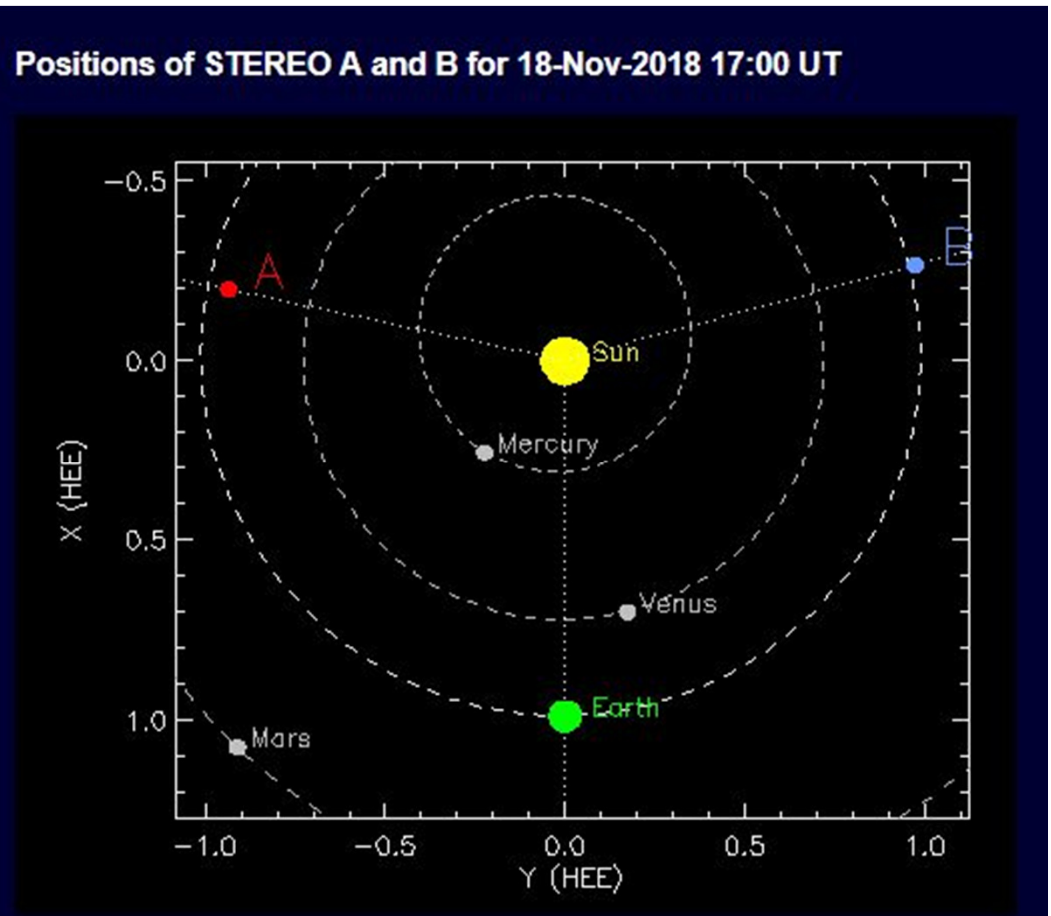
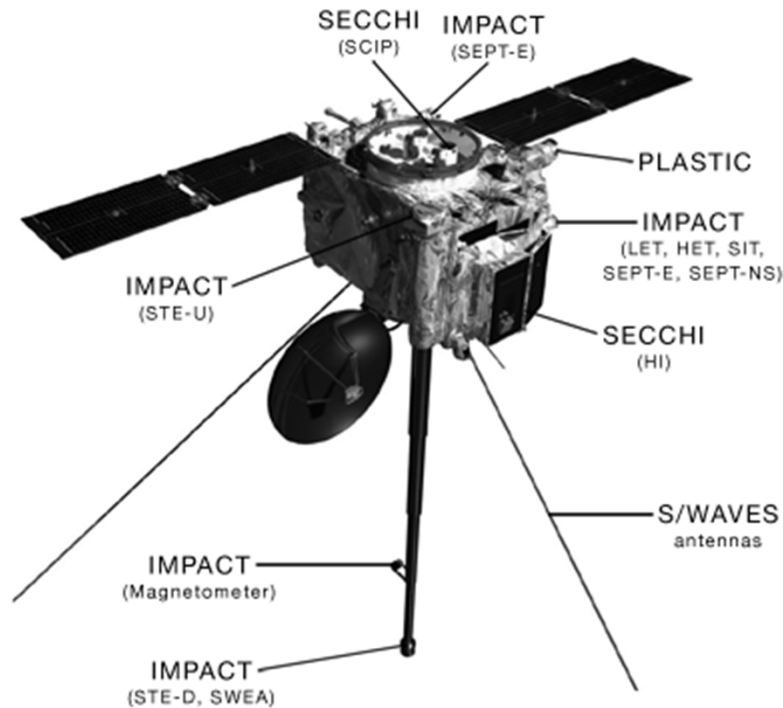
Advanced Composition Explorer (ACE) observes particles of solar, interplanetary, interstellar, and galactic origins, spanning the energy range from solar wind ions to galactic cosmic ray nuclei.

## ACE RTSW (Estimated) MAG &amp; SWEFAM

Begin: 2018-11-17 18:00:00UTC



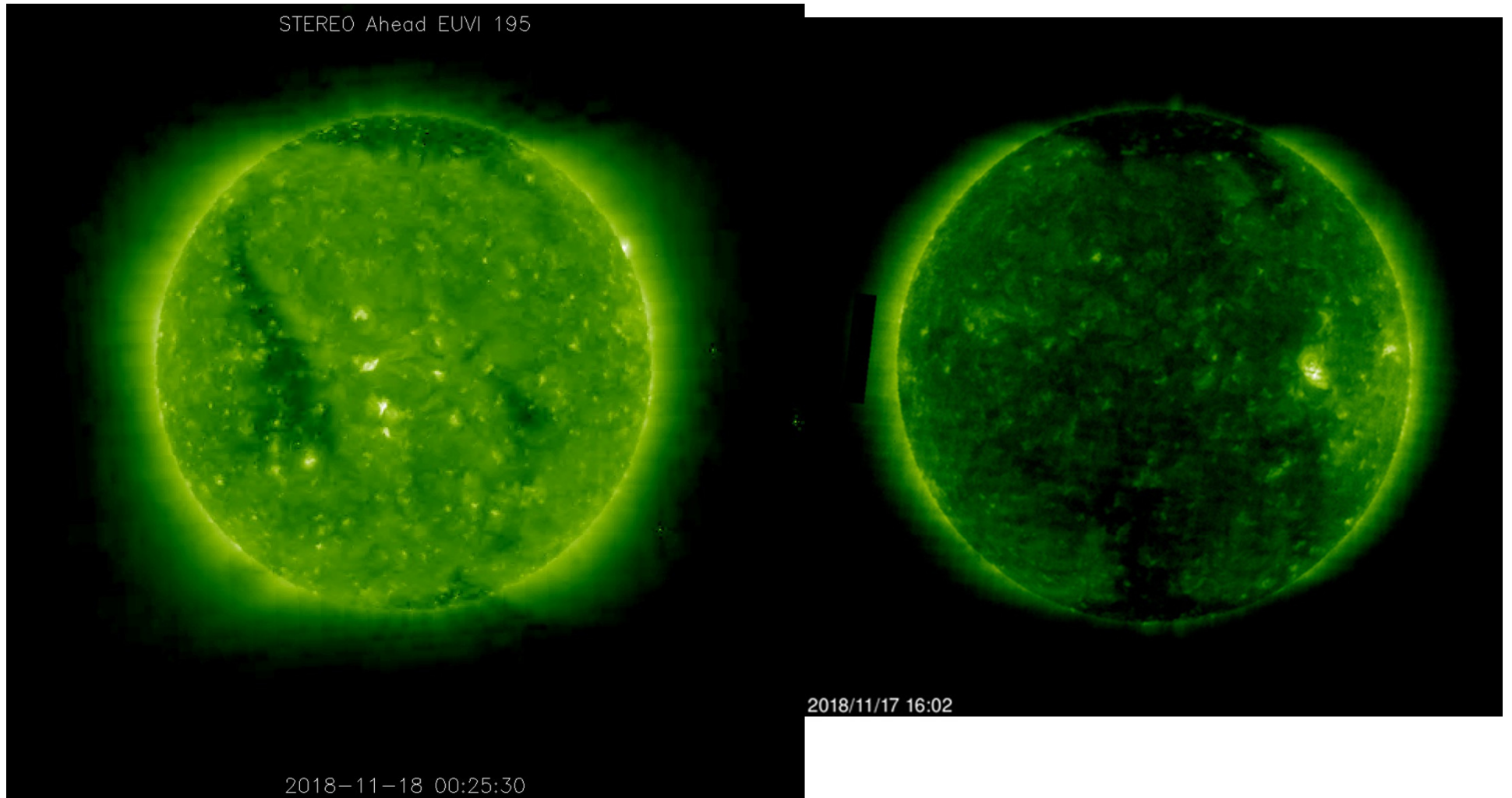
# The Solar Terrestrial Relations Observatory (STEREO). Two Stereo spacecraft observe the solar corona and wind from the far side



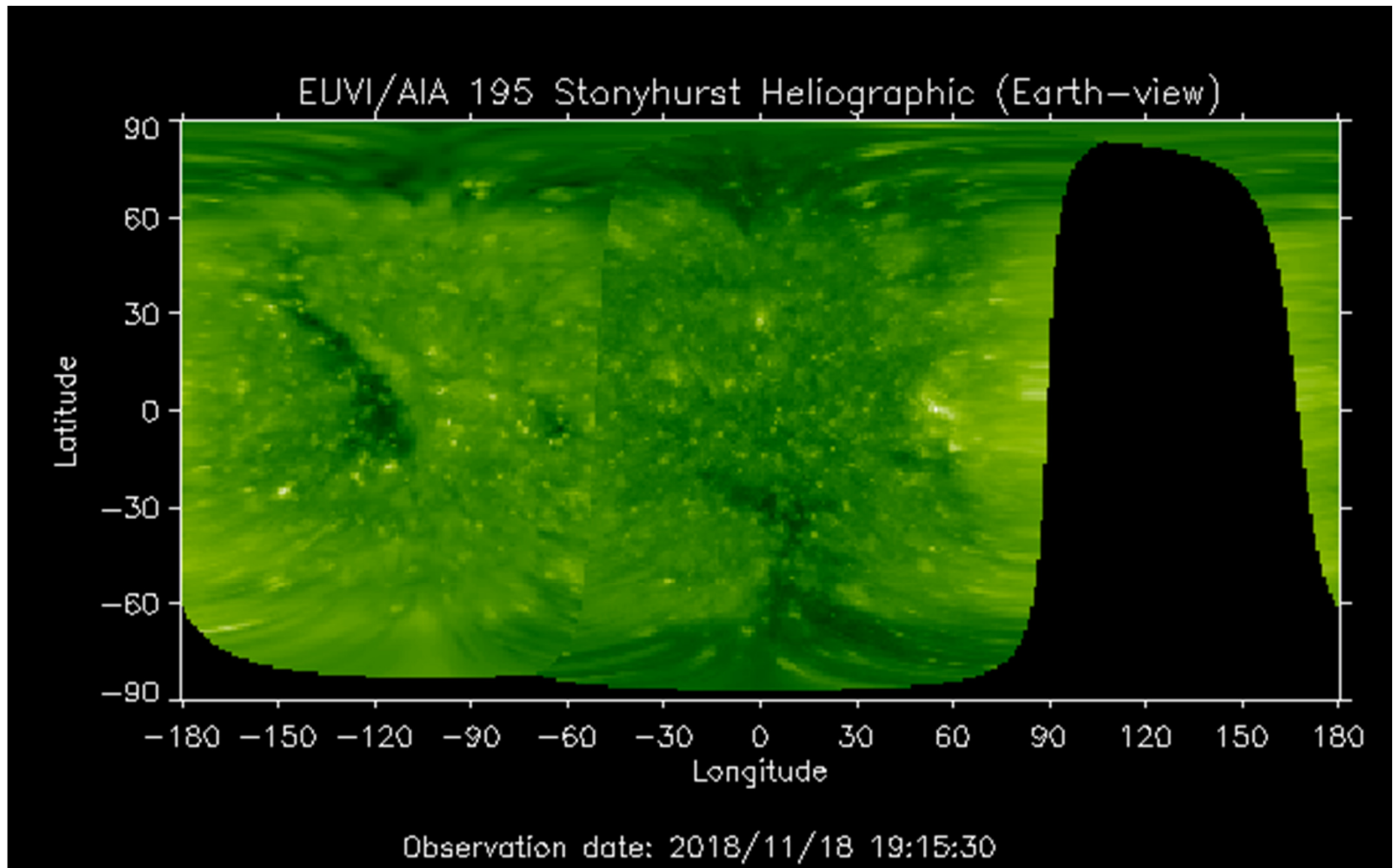
# Images of the solar corona $\lambda=195\text{\AA}$

STEREO A

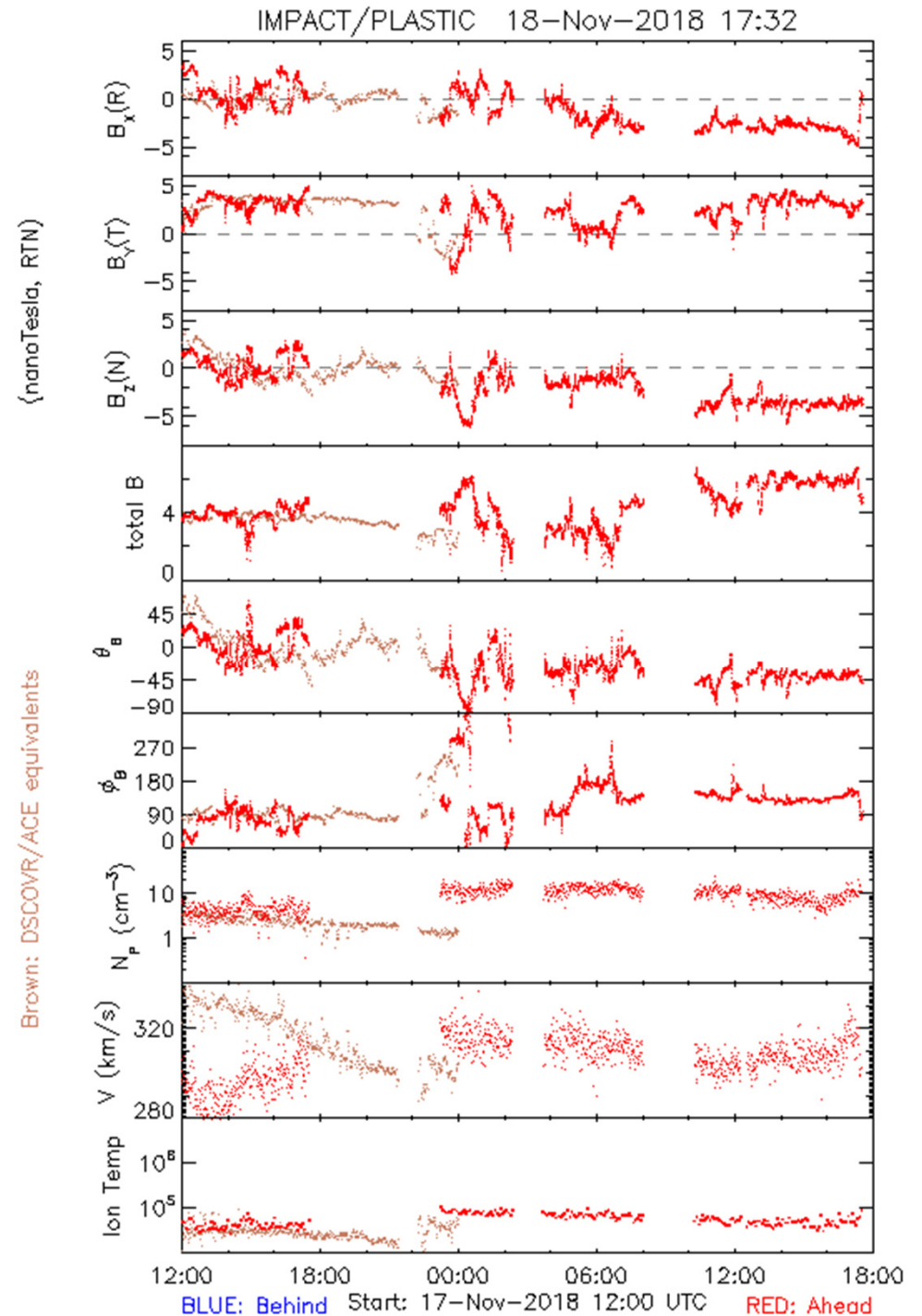
SOHO/EIT



# Combined map of the solar corona



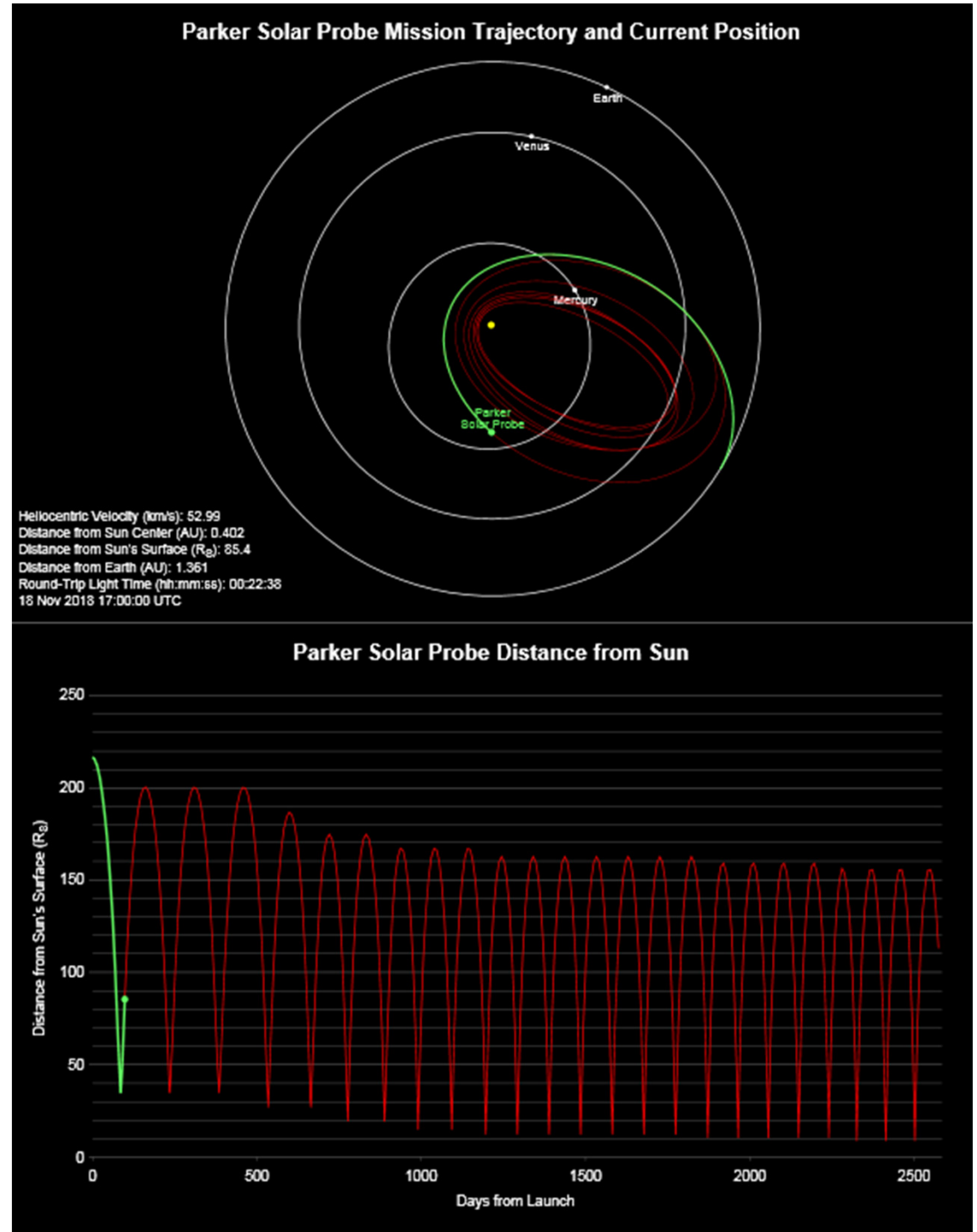
# Solar wind measurements from STEREO/A



# Parker Solar Probe mission

Parker Solar Probe launched on August 12, 2018, has three detailed science objectives:

- Trace the flow of energy that heats and accelerates the solar corona and solar wind.
- Determine the structure and dynamics of the plasma and magnetic fields at the sources of the solar wind.
- Explore mechanisms that accelerate and transport energetic particles.



# Parker Solar Probe Instruments

- **Fields Experiment (FIELDS)**

This investigation will make direct measurements of electric and magnetic fields and waves, Poynting flux, absolute plasma density and electron temperature, spacecraft floating potential and density fluctuations, and radio emissions.

*PI: Prof. Stuart Bale; University of California, Berkeley*

- **Integrated Science Investigation of the sun (IS<sup>☉</sup>IS)**

This investigation makes observations of energetic electrons, protons and heavy ions that are accelerated to high energies (10s of keV to 100 MeV) in the sun's atmosphere and inner heliosphere, and correlates them with solar wind and coronal structures.

*PI: Dr. David McComas; Princeton University*

- **Wide-field Imager for Solar PRobe (WISPR)**

These telescopes will take images of the solar corona and inner heliosphere. The experiment will also provide images of the solar wind, shocks and other structures as they approach and pass the spacecraft. This investigation complements the other instruments on the spacecraft providing direct measurements by imaging the plasma the other instruments sample.

*PI: Dr. Russell Howard; Naval Research Laboratory*

- **Solar Wind Electrons Alphas and Protons (SWEAP) Investigation**

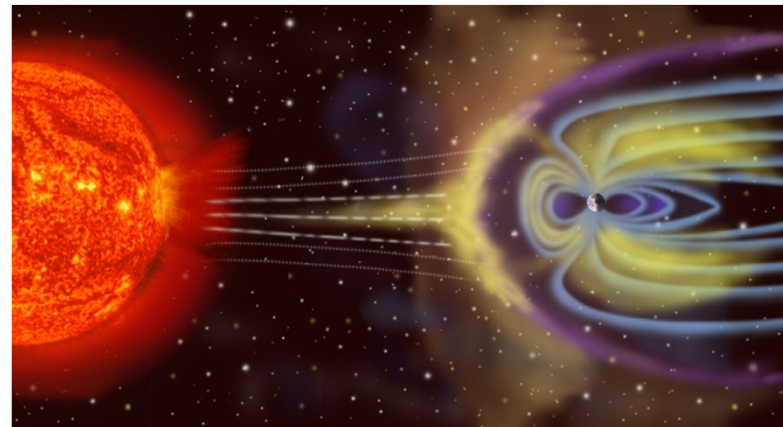
This investigation will count the most abundant particles in the solar wind -- electrons, protons and helium ions - - and measure their properties such as velocity, density, and temperature.

*SWEAP PI: Prof. Justin Kasper; University of Michigan/ Smithsonian Astrophysics Observatory*

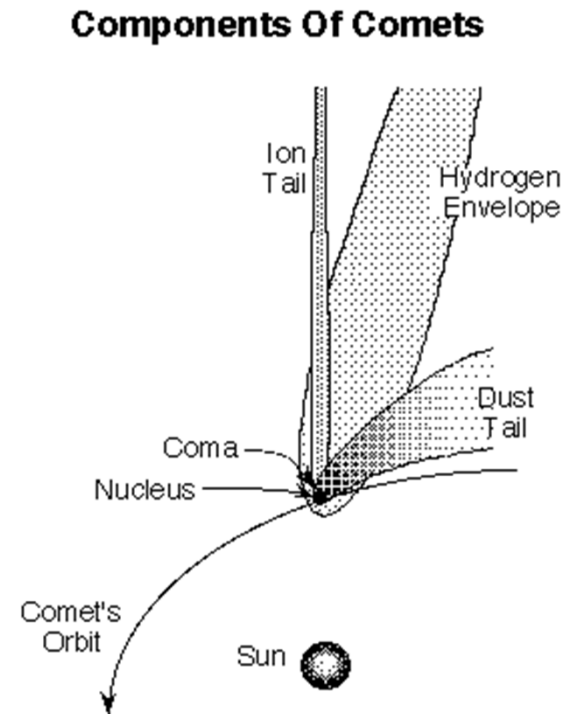
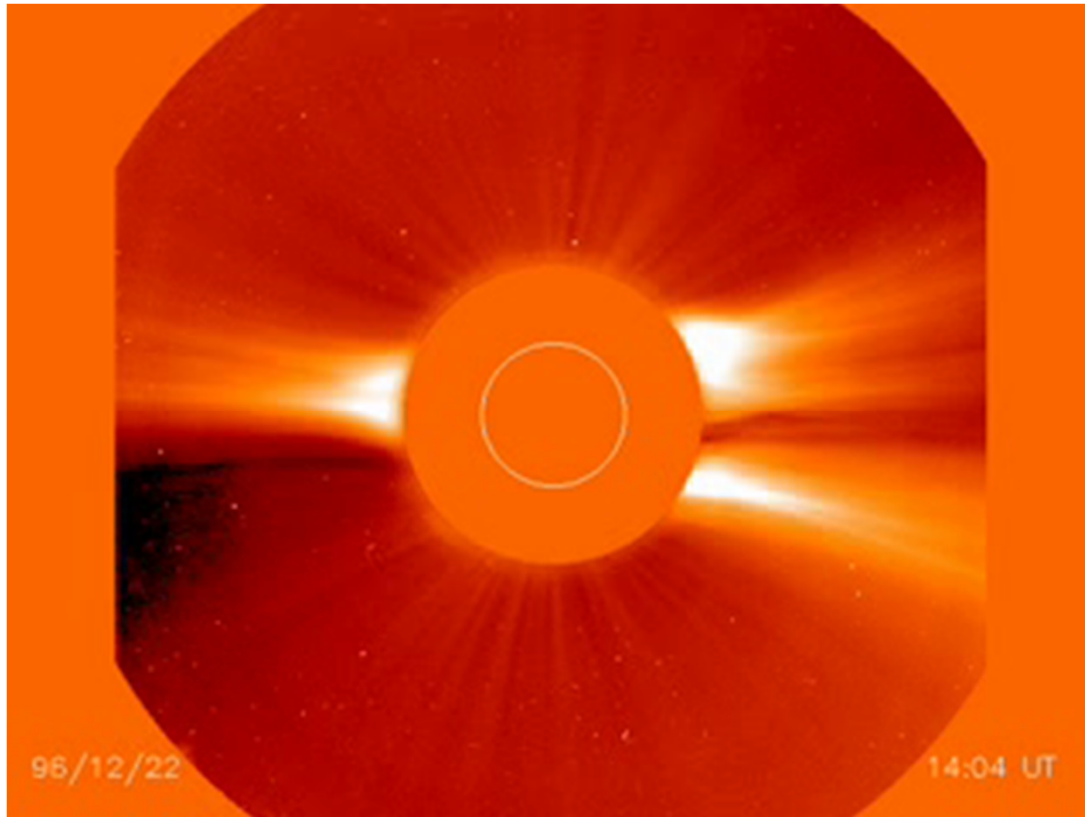
## Expansion of the Solar Corona

Earlier observational suggestions of the existence of the wind were based on the study of solar-terrestrial relations and on the behavior of the tails of comets. In the first half of this century, “solar corpuscular radiation” was commonly invoked to explain auroras and geomagnetic activity, although the radiations were assumed to be associated with solar activity, and were thought to be transient rather than continuous.

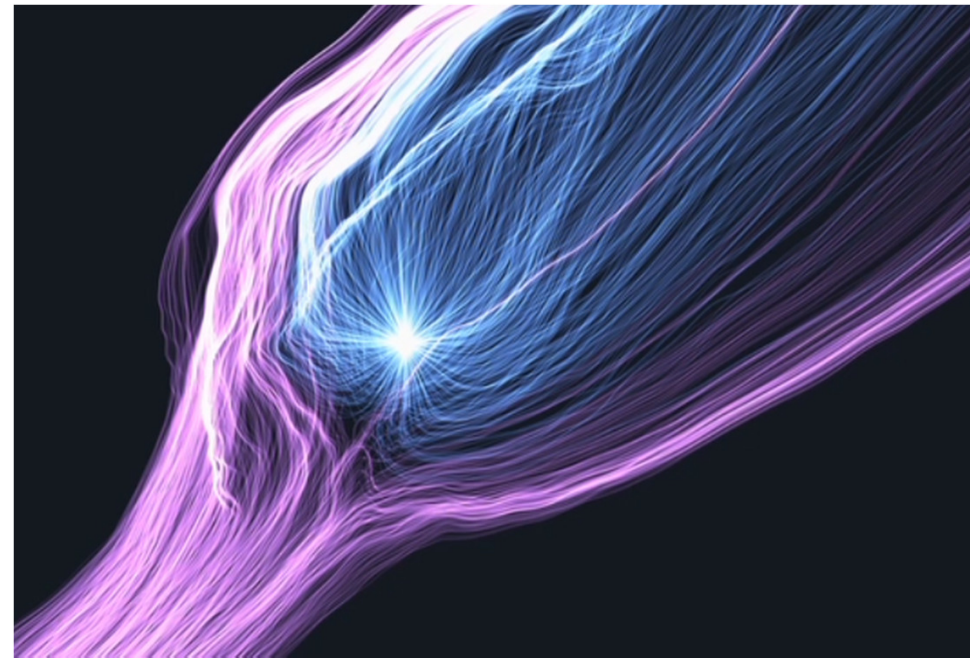
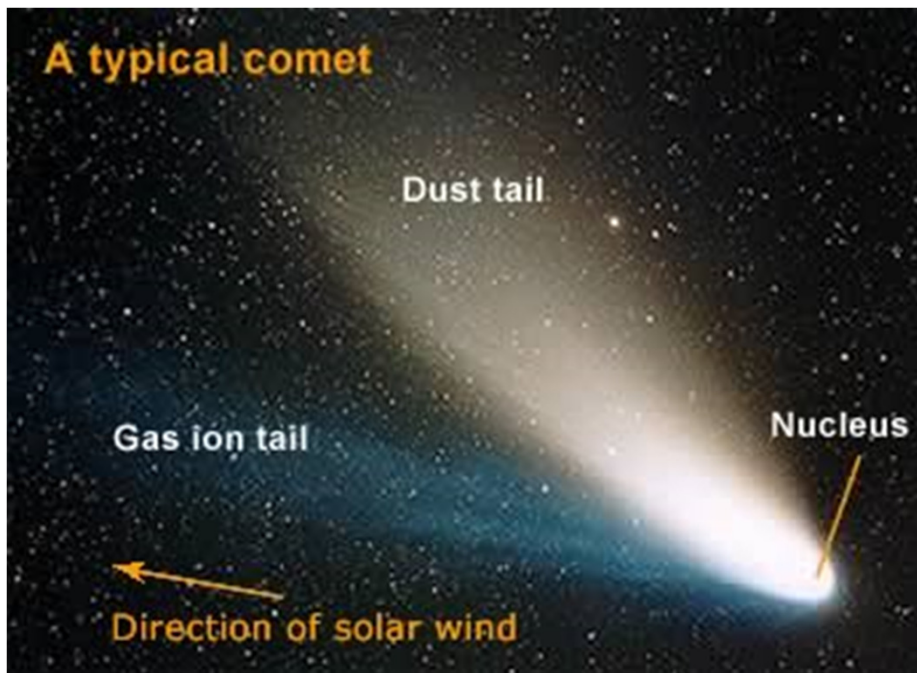
Geomagnetic storms were first noticed in the 19th Century during which the Earth’s magnetic field suddenly increased by about  $10^{-3}$  G and was followed by a slow decay. Normally these geomagnetic storms occurred one or two days after a large solar flare. In addition, it was noticed that flares and geomagnetic activity seemed to have the same 11 year periodicity. Thus, the implication was that there was an electrical connection between the Earth and the Sun.



In the 1950s, Biermann argued that the anti-sunward orientation of the ionized tails of comets was produced by an interplanetary background of ions flowing continuously and radially from the Sun. However, Biermann's model required large velocities and an uncomfortably large density of ions (the comet-wind interaction is now known to be very different from that proposed by Biermann).



## Comet interaction with the solar wind



Gas ion tail is directed along the magnetic field lines in the solar wind. Dust tail follows the comet orbit and deflected by the light pressure.

Numerical simulations of the interaction of the solar wind with 67P/Churyumov-Gerasimenko comet observed by Rosetta spacecraft in August 2014.

Animation illustrating that the solar wind mostly originates from regions with “open” magnetic field lines



# Attempt to construct an expanded model of the solar corona

This suggestion of a connection between the Earth and the Sun led to the idea of an extended corona and in 1957 Chapman presented his model of a hydrostatic corona. The basic idea was to consider an energy equation with only conduction and hydrostatic pressure balance.

Thus, the energy equation: 
$$\frac{\partial T}{\partial t} = \nabla \cdot (\kappa \nabla T)$$

in spherical coordinates, reduces to 
$$\frac{d}{dr} \left( r^2 \kappa \frac{dT}{dr} \right) = 0.$$

The conductivity,  $\kappa$ , in an ionized hydrogen plasma is given by

$$\kappa = \kappa_0 T^{5/2},$$

where  $\kappa_0$  is a constant. Notice how the conductivity depends on temperature. This means that thermal conduction is more efficient at smoothing out temperature variations at higher temperature values.

Thus,

$$r^2 \kappa_0 T^{5/2} \frac{dT}{dr} = C,$$

where  $C$  is a constant. This may be rearranged into the form

$$\frac{2}{7} \frac{d}{dr} (T^{7/2}) = \frac{C}{\kappa_0 r^2},$$

and integrating gives

$$T^{7/2} = -\frac{C}{\kappa_0 r} + D.$$

The constants  $C$  and  $D$  are determined by the boundary conditions on the temperature, namely

$$T = T_0 \text{ at } r = R_\odot, \quad T \rightarrow 0 \text{ as } r \rightarrow \infty.$$

Hence,  $D = 0$  and  $C = -T_0^{7/2} \kappa_0 R_\odot$ , and

$$T = T_0 \left( \frac{R_\odot}{r} \right)^{2/7}.$$

## Analysis of the hydrostatic model of the solar corona

Thus, for a hydrostatic model we obtain the temperature distribution:  $T = T_0 \left( \frac{R_\odot}{r} \right)^{2/7}$ .

Notice that for a “surface”, coronal temperature of  $10^6$  K the temperature of the corona at the Earth,  $1AU = 214R_\odot$ , is about  $10^5$  K. This is actually a little low but does not seem too bad. The main problem with this model appears when hydrostatic pressure balance is considered:

$$\frac{dp}{dr} = -\frac{GM_\odot\rho}{r^2}$$

Applying the gas law  $p = \rho RT$  and  $T$  given by the solution we obtain

$$p = p_0 \exp \left\{ \frac{7GM_\odot\rho_0}{5p_0R_\odot} \left[ \left( \frac{R_\odot}{r} \right)^{5/7} - 1 \right] \right\},$$

where  $p_0$  and  $\rho_0$  are the values of the pressure and density at the solar surface. However, it is clear from that the pressure tends to a constant value as  $r$  tends to infinity. This does not make physical sense. As one tends to large distances away from the Sun the pressure should continue to drop down to the value of the interstellar pressure which is approximately  $10^{-15} p_0$ . In addition, the density tends to infinity for large values of  $r$ . Thus, the hydrostatic model is not physical.

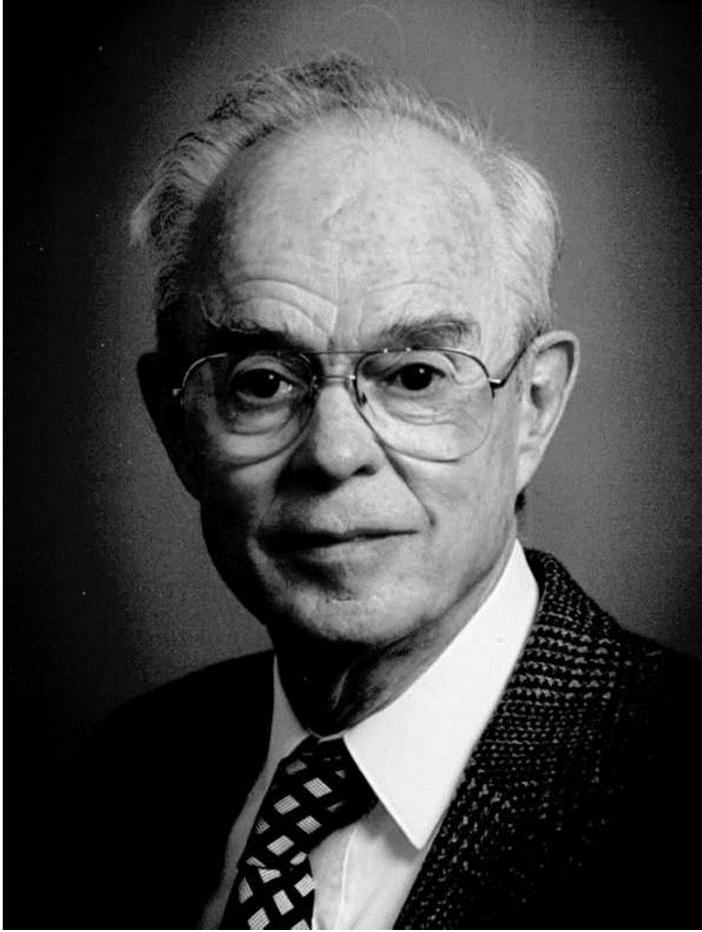
## **Parker's solar wind model**

Parker (1958) suggested that the corona could not remain in static equilibrium but must be continually expanding since the interstellar pressure cannot contain a static corona.

The continual expansion is called the solar wind.

The existence of a solar wind had been known from comet observations but the properties predicted by Parker were confirmed by the satellites Lunik III and Venus I in 1959 and by Mariner II in the early 1960s.

# Eugene N. Parker



Parker realized that this mismatch was not just an artifact of the model but implied that the solar corona could not be in hydrostatic equilibrium out to large distances from the Sun. Motivated also by Biermann's arguments for a continuous, rapid outflow of material from the Sun, Parker began to investigate an alternative solution, a corona in continuous expansion.

Parker developed the theory on the supersonic solar wind and predicted the Parker spiral shape of the solar magnetic field in the outer solar system. In 1987, Parker proposed that the solar corona might be heated by myriad tiny "nanoflares", miniature brightenings resembling solar flares that would occur all over the surface of the Sun.

# Parker's theory of the solar wind

The main assumptions of Parker's model are that the outflow is steady, spherically symmetric and isothermal. It is straightforward to relax the isothermal assumption and consider an adiabatic or polytropic atmosphere.

The basic steady ( $\partial \dots / \partial t = 0$ ) equations are:

$$\nabla \cdot (\rho \mathbf{v}) = 0, \text{ - continuity equations (conservation of mass)}$$

$$\rho (\mathbf{v} \cdot \nabla) \mathbf{v} = -\nabla p + \rho \mathbf{g}, \text{ - momentum equation}$$

$$p = \rho RT, \text{ - equation of state (ideal gas law)}$$

and we assume the temperature is constant:  $T = T_0$ .

The velocity is taken as purely radial so that  $\mathbf{v} = v \hat{\mathbf{r}}$  and gravitational acceleration obeys the inverse square law,  $\mathbf{g} = -GM_{\odot}/r^2$ .

In spherical coordinates and assuming a steady flow,

$$\nabla \cdot (\rho \mathbf{v}) \equiv \frac{d}{dr} (r^2 \rho v) = 0 \quad \Rightarrow \quad r^2 \rho v = \text{const.}$$

and the radial component of momentum equation becomes

$$\rho v \frac{dv}{dr} = -\frac{dp}{dr} - \frac{GM_{\odot} \rho}{r^2}.$$

Defining the isothermal sound speed as  $(p/\rho)^{1/2} = c_s$ ,

the gas law 
$$p = c_s^2 \rho,$$

we get 
$$\rho v \frac{dv}{dr} = -c_s^2 \frac{d\rho}{dr} - \frac{GM_{\odot} \rho}{r^2}.$$

Then dividing by  $\rho$  we obtain: 
$$v \frac{dv}{dr} = -\frac{c_s^2}{\rho} \frac{d\rho}{dr} - \frac{GM_{\odot}}{r^2}.$$

From  $r^2 \rho v = \text{const}$  : 
$$\frac{1}{\rho} \frac{d\rho}{dr} = r^2 v \frac{d}{dr} \left( \frac{1}{r^2 v} \right)$$

Now we can use the continuity equation to express  $d\rho/dr$  and  $\rho$  in terms of  $r^2v$  :

$$v \frac{dv}{dr} = -c_s^2 r^2 v \frac{d}{dr} \left( \frac{1}{r^2 v} \right) - \frac{GM_\odot}{r^2}.$$

Expanding the pressure gradient term and rearranging gives the final radial equation of motion as

$$\left( v - \frac{c_s^2}{v} \right) \frac{dv}{dr} = 2 \frac{c_s^2}{r^2} (r - r_c),$$

where  $r_c = GM_\odot / 2c_s^2$ .

We can see that at  $r = r_c$  velocity is equal to the sound speed:  $v = c_s$ .

Thus,  $r = r_c$  is a critical point. If the velocity of the plasma reaches the sound speed then the radius must either equal  $r_c$  or else the velocity gradient becomes infinite. Another way of saying this is to say that if  $r = r_c$  then either  $dv/dr = 0$  or  $v = c_s$  and if  $v = c_s$  then either  $dv/dr = \infty$  or  $r = r_c$ .

$$\left( v - \frac{c_s^2}{v} \right) \frac{dv}{dr} = 2 \frac{c_s^2}{r^2} (r - r_c)$$

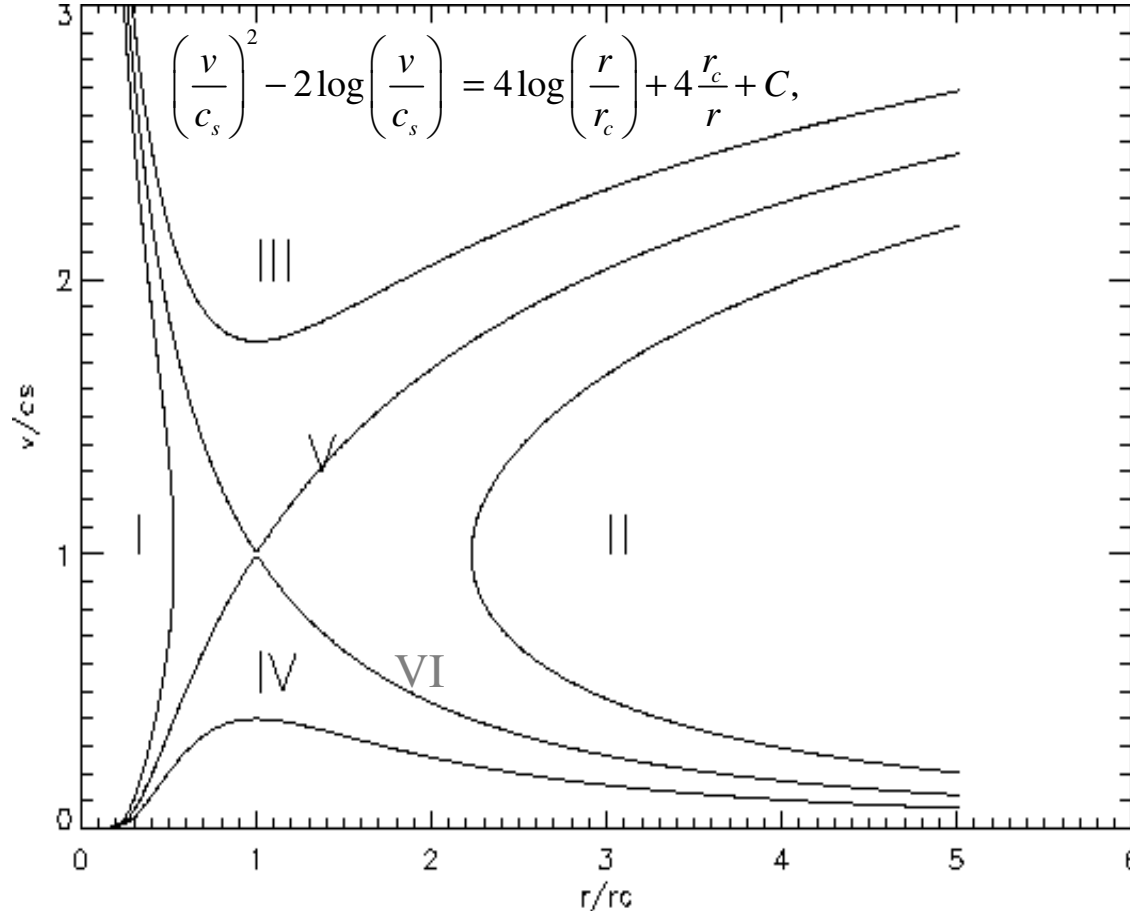
This equation can be integrated to give a transcendental equation for the velocity in terms of the radius as

$$\left( \frac{v}{c_s} \right)^2 - 2 \log \left( \frac{v}{c_s} \right) = 4 \log \left( \frac{r}{r_c} \right) + 4 \frac{r_c}{r} + C,$$

where  $C$  is a constant.

The ODE solutions for  $v/c_s$  can be plotted as a function of  $r/r_c$  for various values of constant  $C$ .

## For various values of C we get six different types of solutions



**Solution I** is double valued and so is unphysical. It is not possible for the plasma to leave the solar surface with a velocity below the sound speed, reach a maximum radius below  $r_c$  and then turn round and return to the Sun with a super-sonic speed.

**Solution II** is also double valued but it never even starts from the solar surface and it is also unphysical.

**Solution III** starts with a velocity greater than the sound speed but such a fast steady outflow is not observed. Hence, this solution must also be neglected.

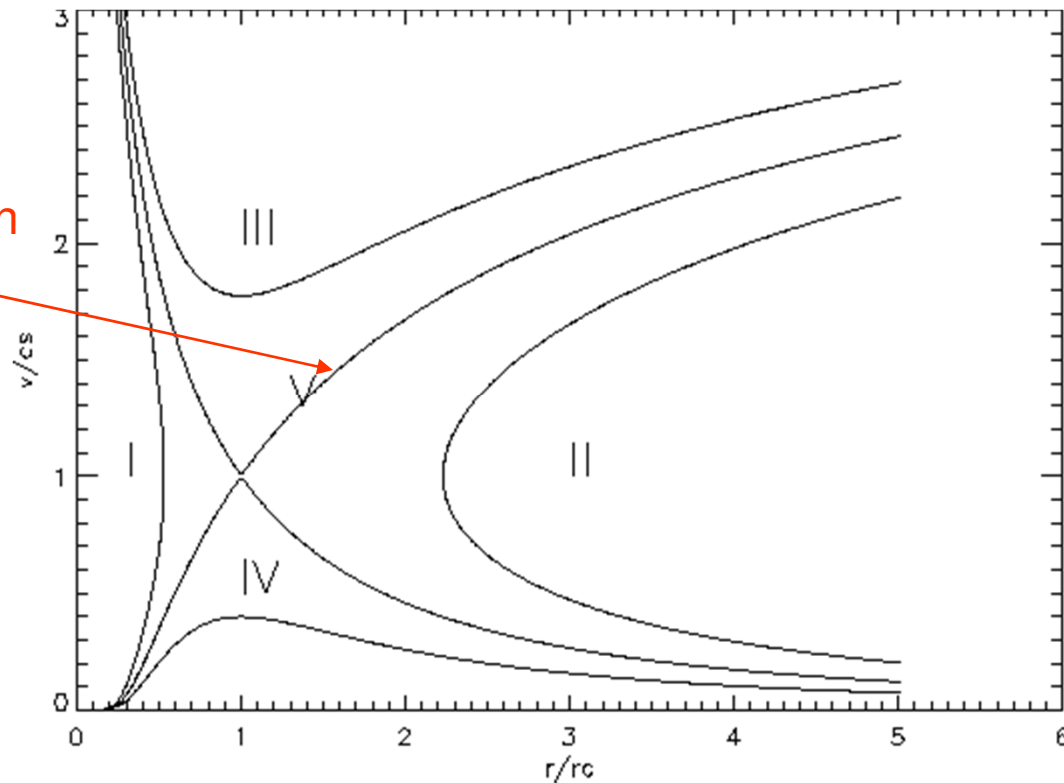
**Solution IV** always remains below the sound speed and is called the **solar breeze solution**.

**Solution V** is the particular case where the plasma leaves the solar surface with a particular speed and passes through the critical point (also called the sonic point) at  $r = r_c$  and  $v = c_s$ . (**solar wind solution**)

For solution V we choose the constant  $C$  so that  $r = r_c$  and  $v = c_s$  and this requires  $C = -3$ .

Is it possible to decide between solutions IV and V?

Solar wind solution



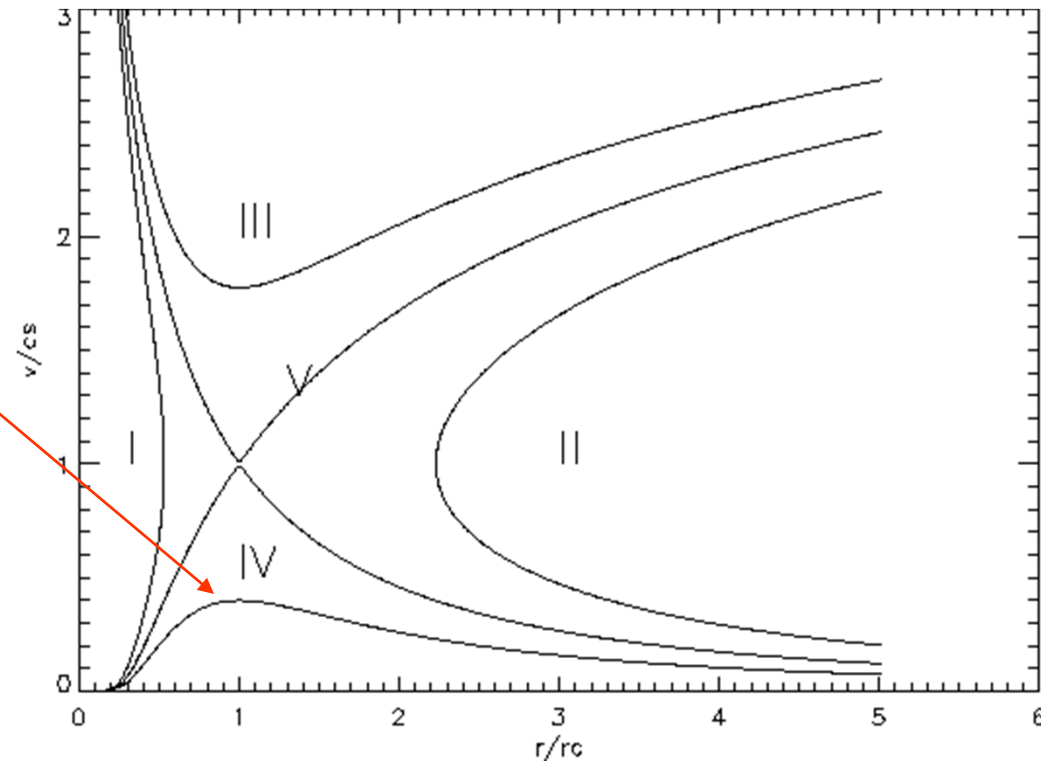
The behavior of solution V for large  $r$  can be obtained quite easily. If  $v \gg c_s$  then

$$\left(\frac{v}{c_s}\right)^2 \approx 4 \log\left(\frac{r}{r_c}\right) \rightarrow \frac{v}{c_s} \approx 2 \left(\log\left(\frac{r}{r_c}\right)\right)^{1/2}.$$

Hence, from the continuity equation the density is given by  $\rho = \frac{\text{const.}}{r^2 v} \approx \frac{\text{const.}}{r^2 \sqrt{\log(r/r_c)}}$ .

Thus,  $\rho$  tends to zero as  $r$  tends to infinity. Since the plasma is isothermal the pressure also tends to zero. This means that the solution can eventually match onto the interstellar plasma at large distances from the Sun. Thus, solution V is a physically realistic model of the solar wind. It predicts that the plasma will be super-sonic beyond the critical point.

Solar breeze solution

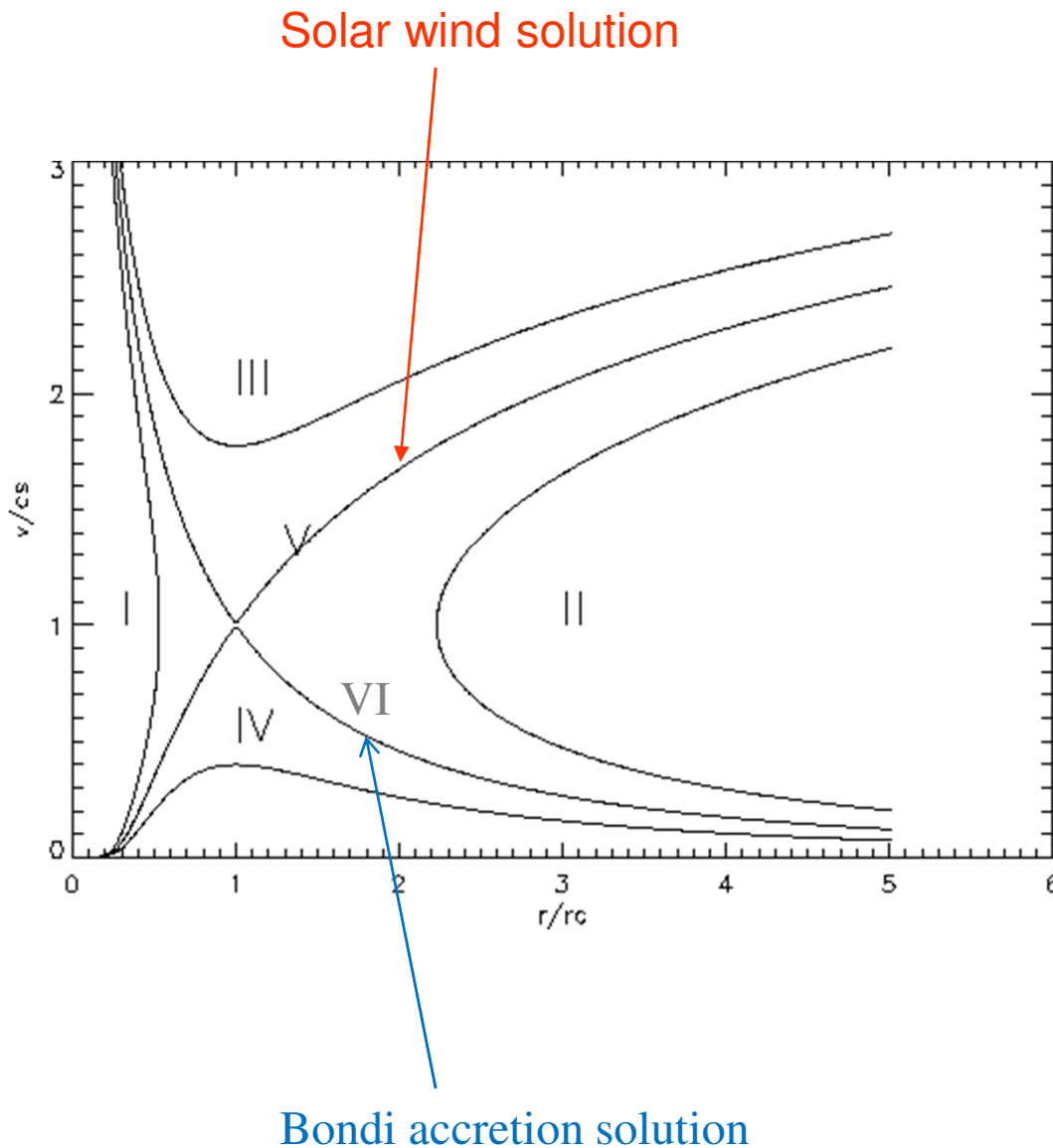


The behavior of solution IV for large  $r$  is quite different. Again from the figure, we see that  $v$  tends to zero as  $r$  tends to infinity. Thus, the solution may now be approximated by

$$-2 \log \left( \frac{v}{c_s} \right) \approx 4 \log \left( \frac{r}{r_c} \right) \rightarrow \frac{v}{c_s} \approx \left( \frac{r_c}{r} \right)^2.$$

The mass continuity equation gives the density as  $\rho = \frac{\text{const.}}{r_c^2 c_s}$ .

Since the density tends to a constant value so will the pressure. Thus, the solar breeze solution is unphysical since it cannot be contained by the extremely small interstellar pressure.



Thus, the Parker solar wind model is given by solution V.

The plasma starts at the solar surface with a small velocity that increases towards the critical point.

At the critical point the speed reaches the sound speed.

Then the flow becomes (and remains) super-sonic while the gas pressure decreases.

## Parameters of the Parker's solar wind solution

We can calculate the critical radius,  $r_c$ . The radius of the Sun is 696 Mm.

Assuming a typical coronal temperature of  $10^6$  K the sound speed is

$$c_s = (RT)^{1/2} = (8.3 \times 10^7 \times 10^6)^{1/2} \approx 10^7 \text{ cm/s} \approx 10^5 \text{ m/s}.$$

The critical radius is  $r_c = \frac{GM_\odot}{2c_s^2} = 7 \times 10^9 \text{ m} \approx 10R_\odot$ .

To put this into context, the radius of the Earth's orbit is  $R_E \approx 214R_\odot$ . Thus, the solar wind is highly super-sonic by the time it reaches the Earth. To calculate the actual wind speed from Parker's model we set  $r = R_E$  and solve for  $v$ . Hence,

$$\left(\frac{v}{c_s}\right)^2 - 2\log\left(\frac{v}{c_s}\right) = 4\log\left(\frac{214}{10}\right) + 4\frac{10}{214} - 3 = 9.44.$$

This may be solved using the Newton-Raphson method (or use Wolfram Alpha) to give

$$v = 3.45c_s = 310 \text{ km s}^{-1}.$$

Observations at 1AU give the quiet solar wind as  $v \approx 320 \text{ km s}^{-1}$ .

Thus, Parker's solar wind model gives quite a good estimation of the velocity.

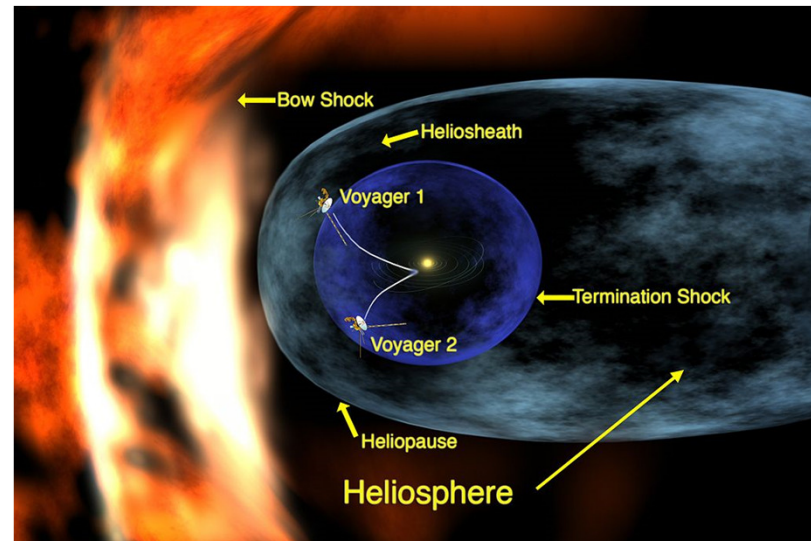
Some notes:

1. As an alternative energy equation it is possible to use a polytrope of the form:  $p = K\rho^\gamma$ .

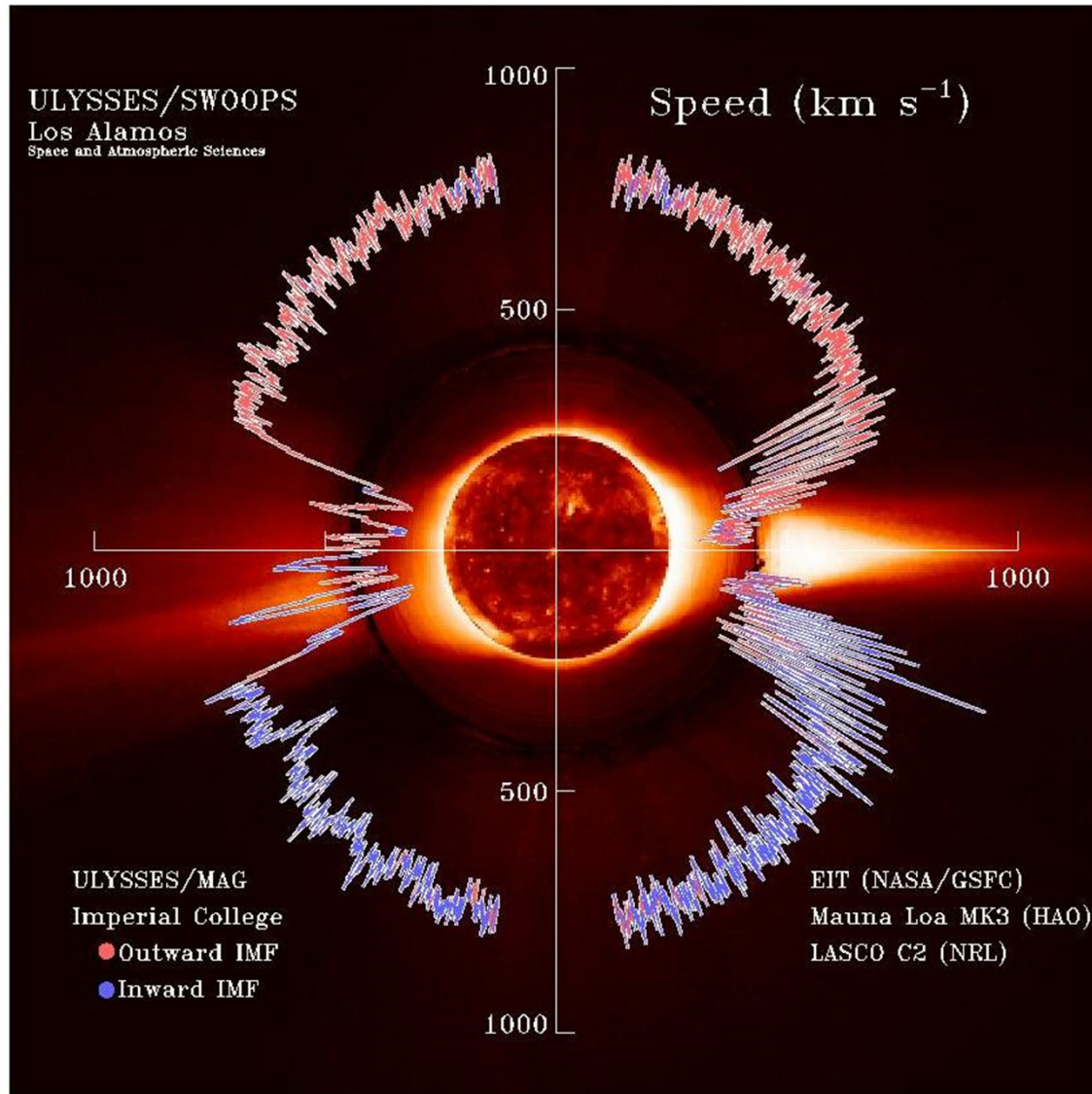
2. The real solar wind does not come from the whole of the solar surface but only from the regions where the magnetic field is open. This is only about 20 percent of the whole surface. The strong magnetic field of the other 80 percent is closed and effectively holds in the hot corona.

3. The total number of particles carried away from the Sun by the solar wind is about  $1.3 \times 10^{36}$  per second. Thus, the total mass loss each year is about  $(2-3) \times 10^{-14}$  solar masses, or about one billion kilograms per second.

4. The solar wind probably ends in a shock called the heliopause at about  $100AU$ .



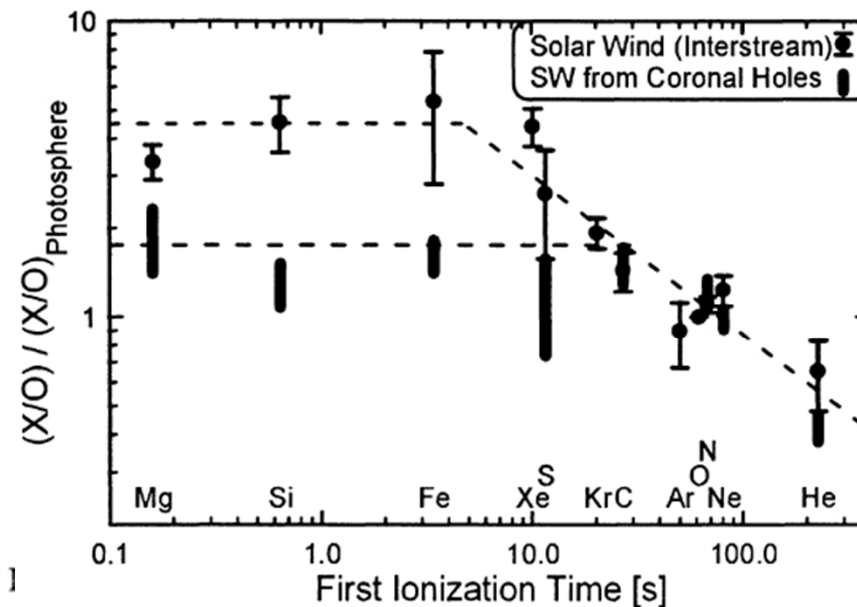
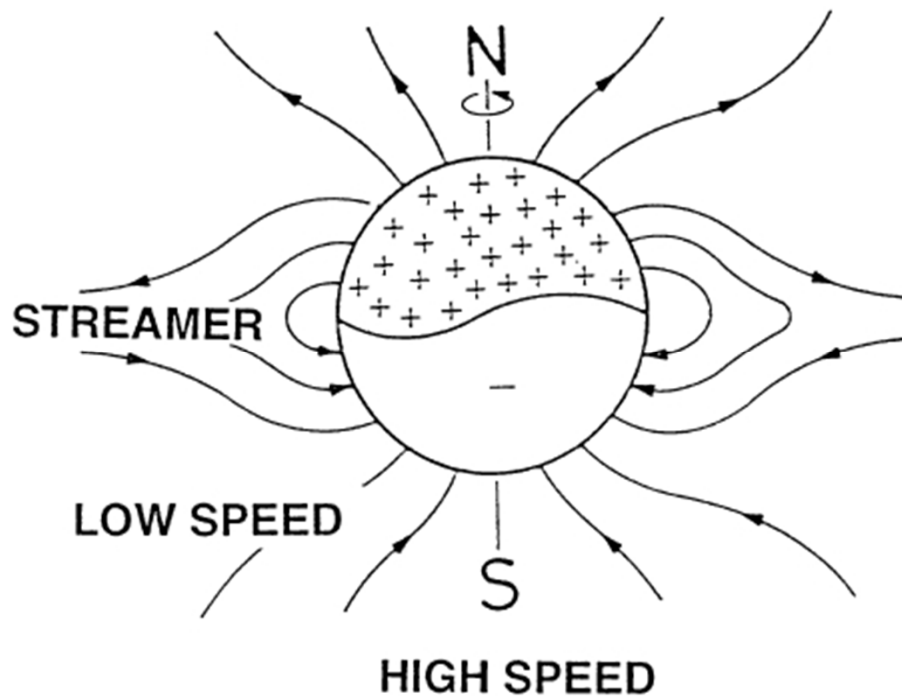
## Fast and slow solar wind



Measurements of the solar wind speed from the Ulysses spacecraft. It passed over the Sun's south and north poles. Its measurements of the solar wind speed, magnetic field strength and direction, and composition have provided us with a new view of the solar wind. The data show that the solar wind is not uniform. Although it is always directed away from the Sun, it changes speed and carries with it magnetic clouds, interacting regions where high speed wind catches up with slow speed wind, and composition variations. The solar wind speed is high (800 km/s) over coronal holes and slow (300 km/s) over streamers.

Composition of the fast and slow wind is different because of the “First Ionization Potential” effect – due to magnetic fields and different ionization times of ions.

# First Ionization Potential (FIP) Effect in Fast and Slow Wind



Elemental abundances in the solar wind as a function of their “first ionisation time”

Sketch of the solar wind expansion in the dipole geometry of the Sun’s magnetic field (corresponding to the solar minimum conditions)

“First Ionization Potential” (FIP) effect  
Abundances of various elements relative to the photospheric abundances in the fast and slow wind vs. a characteristic ionization time.

(Geiss et al, 1995)

# Interplanetary Magnetic Field (IMF)

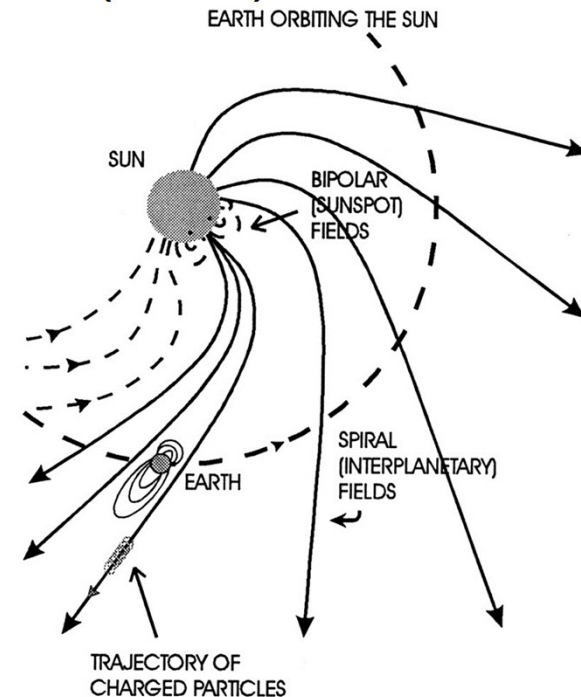
The interplanetary magnetic field (IMF) is a part of the Sun's magnetic field that is carried into interplanetary space by the solar wind.

The interplanetary magnetic field lines are said to be "frozen in" to the solar wind plasma.

Because of the Sun's rotation, the IMF, like the solar wind, travels outward in a spiral pattern.

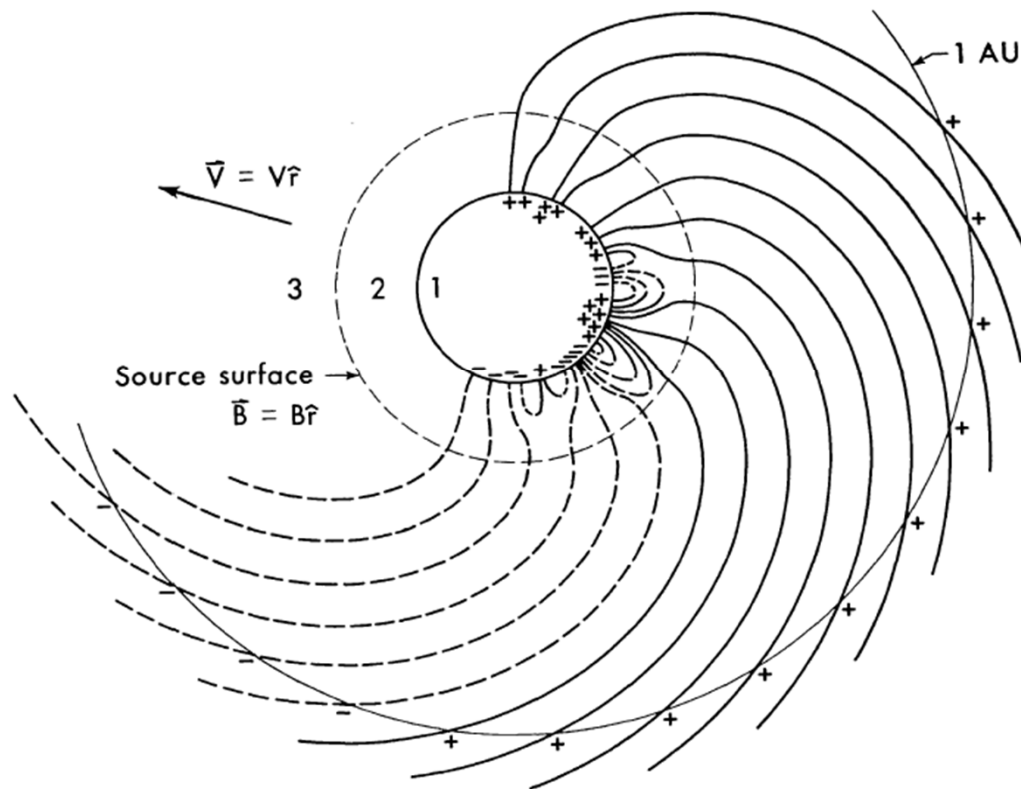
The IMF originates in regions on the Sun where the magnetic field is "open"—that is, where field lines emerging from one region do not return to a conjugate region but extend virtually indefinitely into space.

The direction (polarity, sense) of the field in the Sun's northern hemisphere is opposite that of the field in the southern hemisphere. (The polarities reverse with each solar cycle.)



## Magnetic Effects. Source-Surface Model.

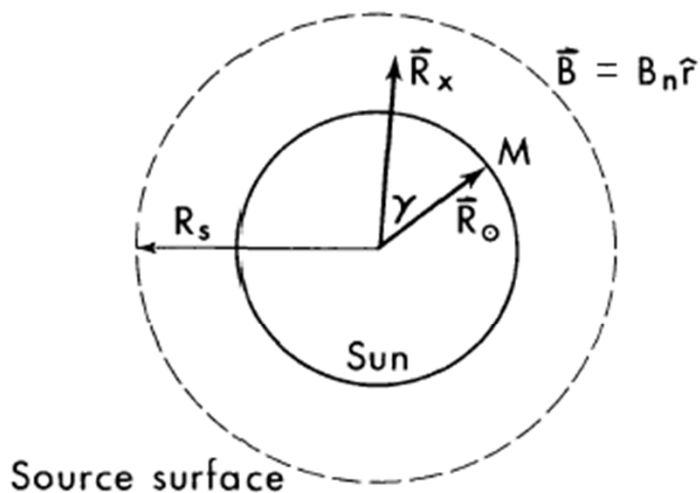
The interplanetary magnetic field has a sector structure (Ness and Wilcox, 1964). Sources for the magnetic field are related to the observed photospheric field and to the field computed at a 'source' surface about  $1.5 R_{\odot}$  above the photosphere. The large-scale interplanetary magnetic field sector pattern is related to the field pattern at this 'source' surface.



Schatten et al (1969)

**Schematic presentation of the sector magnetic structure and the source surface model. The photospheric field is measured in region 1. Closed field lines (loops) exist in region 2. The field in this region is calculated from potential theory. Currents flowing near the source surface eliminate the transverse component of the magnetic field, and the solar wind extends the source surface magnetic field into interplanetary space. The magnetic field is then observed by spacecraft at 1AU.**

## GREEN'S FUNCTION SOLUTION OF MAGNETIC FIELD INSIDE SOURCE SURFACE



Source of field lines  
of strength  $M$  at  
position  $\vec{R}_\odot$  or  $\theta', \phi'$  on sun

Potential at  $\vec{R}_x =$

$$\Phi(\vec{R}_x) = \frac{M}{|\vec{R}_x - \vec{R}_\odot|} - \frac{M R_s / R_\odot}{|\vec{R}_x - \vec{R}_\odot R_s^2 / R_\odot^2|}$$

$$\vec{B}(\vec{R}_x) = -\nabla \Phi$$

Magnetic field due to source  $M$

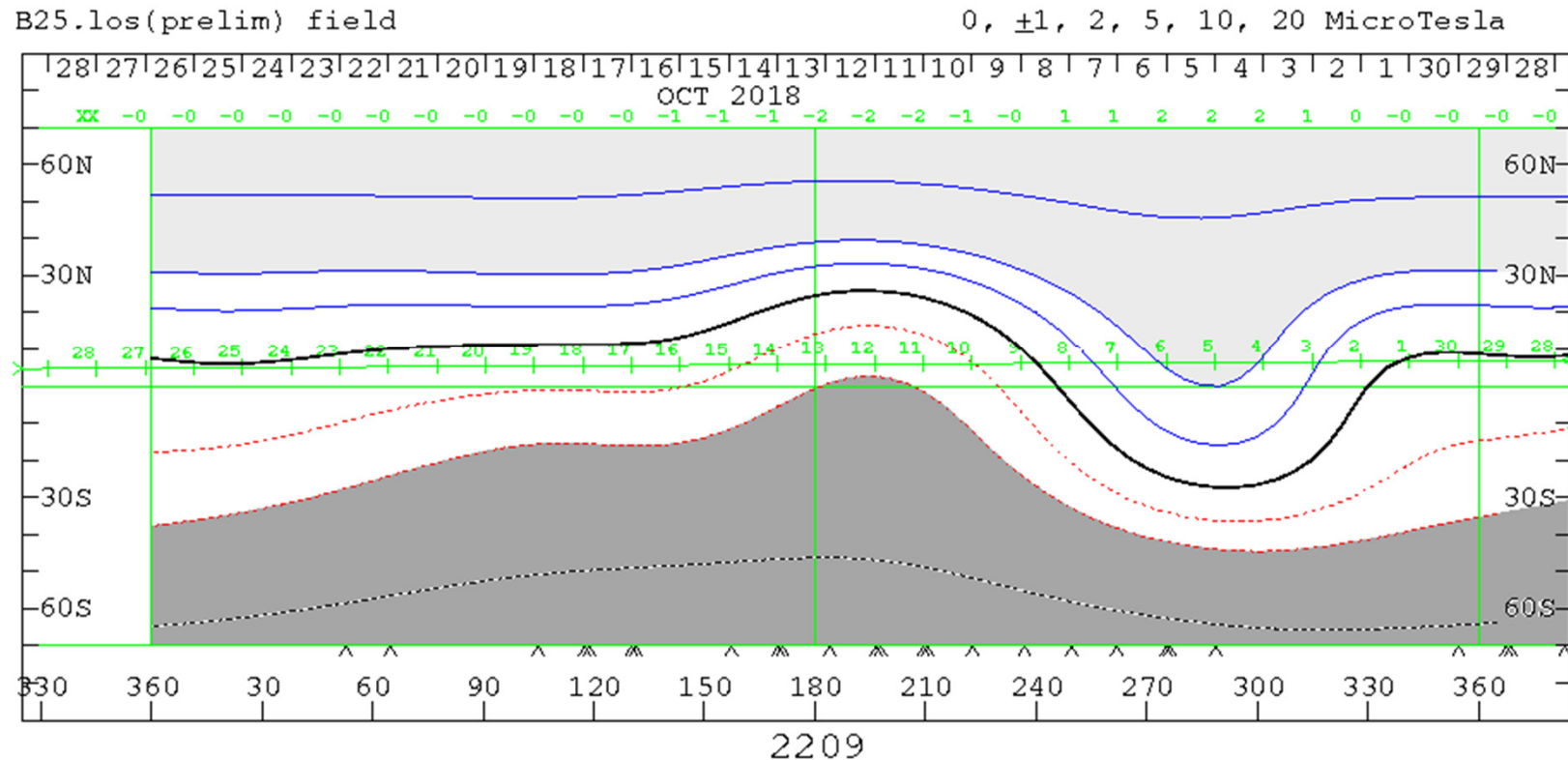
$$\vec{B}_n = -\frac{M \hat{r}}{R_s^2} \frac{R_s}{R_\odot} \left(1 - \frac{R_s^2}{R_\odot^2}\right) \left/ \left(1 + \frac{R_s^2}{R_\odot^2} - \frac{2R_s}{R_\odot} \cos \gamma\right)^{3/2}\right.$$

Magnetic field due to  
distribution of sources

$$\vec{B}_n(\theta, \phi; R_s) = \int \vec{B}_n(\theta, \phi, \theta', \phi'; R_s) \cdot M(\theta', \phi') d\Omega'$$

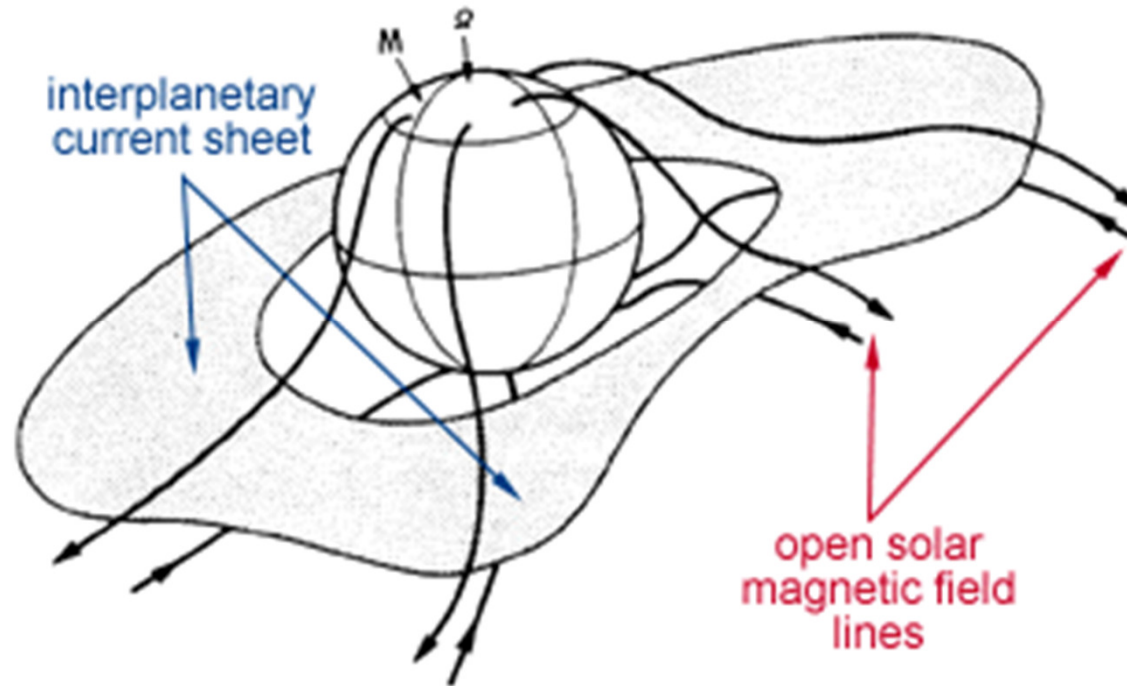
**The potential solution for the magnetic field produced by a source of field lines with a normal magnetic field boundary is shown. The magnetic field on the source surface is also calculated.**

## Wilcox Solar Observatory Source Surface Field Map in Carrington coordinates.



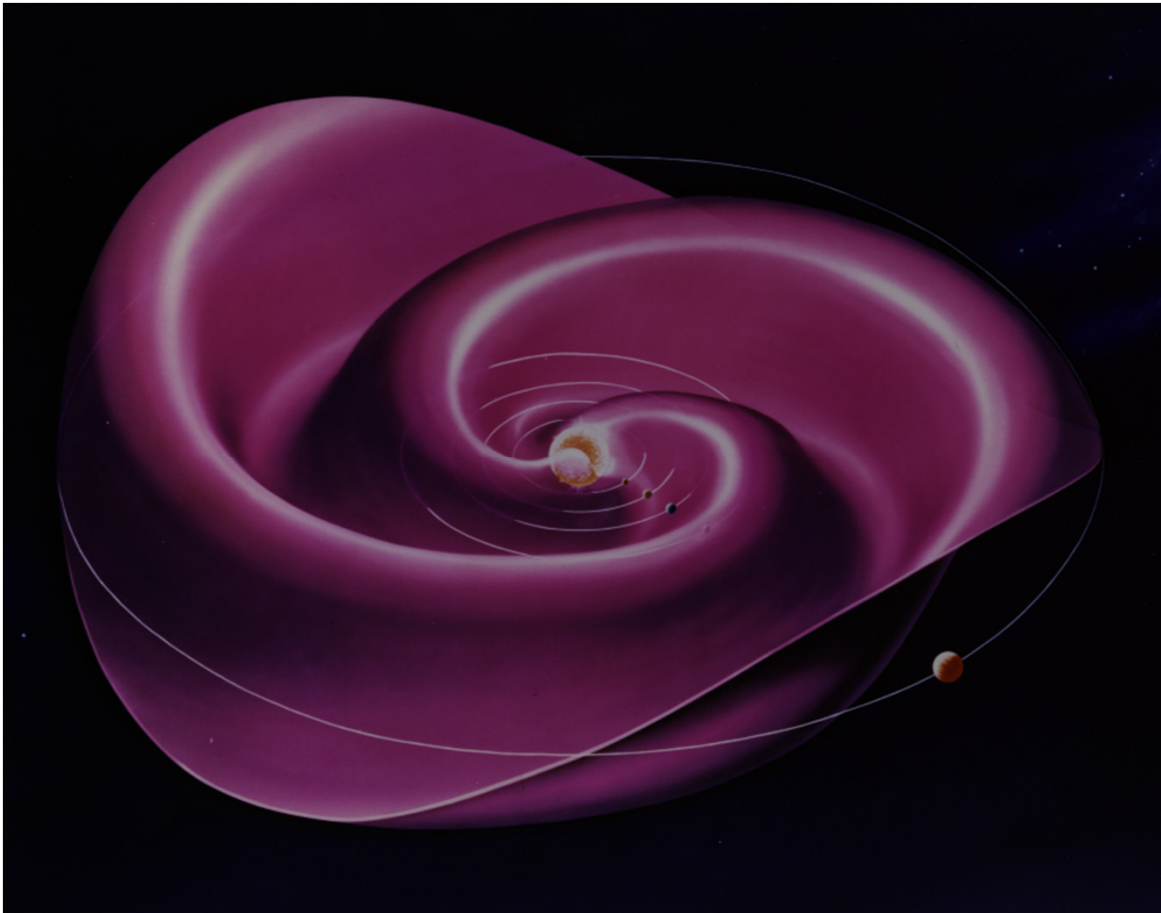
The coronal magnetic field is calculated from photospheric field observations with a potential field model. The field is forced to be radial at the source surface to approximate the effect of the accelerating solar wind on the field configuration. The \*classic\* model locates the source surface at 2.5 solar radii, assumes that the photospheric field has a meridional component and requires a somewhat ad hoc polar field correction to closely match the observations of the IMF at Earth. The dark and light areas show the distribution of magnetic field of the opposite polarities. The sector structure is determined by the neutral surface separating these polarities. The gradient of magnetic field across the neutral surface corresponds to heliospheric current sheet (<http://wso.Stanford.EDU/>)

## Heliospheric Current Sheet



Along the plane of the Sun's magnetic equator, the oppositely directed open field lines run parallel to each other and are separated by a thin current sheet known as the "**interplanetary current sheet**" or "**heliospheric current sheet**". The current sheet is tilted (because of an offset between the Sun's rotational and magnetic axes) and warped (because of a quadrupole moment in the solar magnetic field) and thus has a wavy, "ballerina skirt"-like structure as it extends into interplanetary space (see the figure on the next page). Because the Earth is located sometimes above and sometimes below the rotating current sheet, it experiences regular, periodic changes in the polarity of the IMF. These periods of alternating positive (away from the Sun) and negative (toward the Sun) polarity are known as **magnetic sectors**.

## Artist's Conception of the Heliospheric Current Sheet



The heliospheric current sheet separates regions of the solar wind where the magnetic field points toward or away from the Sun.

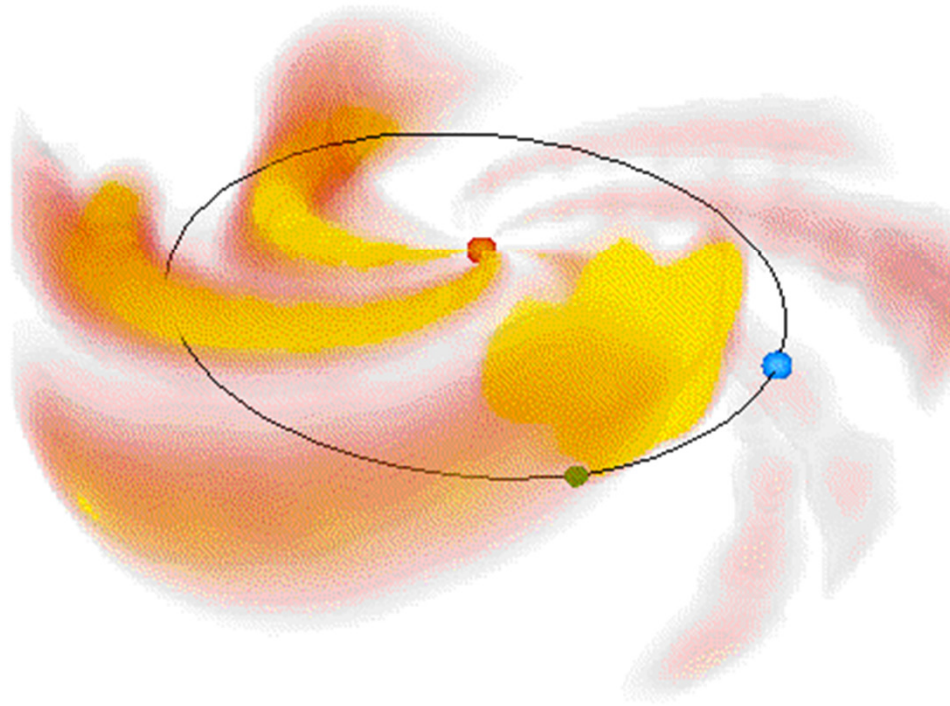
The complex field structure in the photosphere simplifies with increasing height in the corona until a single line separates the two polarities at about 2.5 solar radii.

That line is drawn out by the radially accelerating solar wind to form a surface similar to the one shown in this idealized picture.

The surface is curved because the underlying magnetic pattern rotates every 27 days with the Sun.

It would take about 3 weeks for material near the current sheet traveling at 400 km/s in the solar wind to reach the orbit of Jupiter, as depicted

## Illustration of the spiral structure disrupted by a CME



The shape of the current sheet usually evolves slowly - over months - as the large-scale pattern of the Sun's field changes in response to the emergence and decay of solar active regions.

Coronal mass ejections often disrupt the background pattern temporarily, but sometimes the changes are permanent.

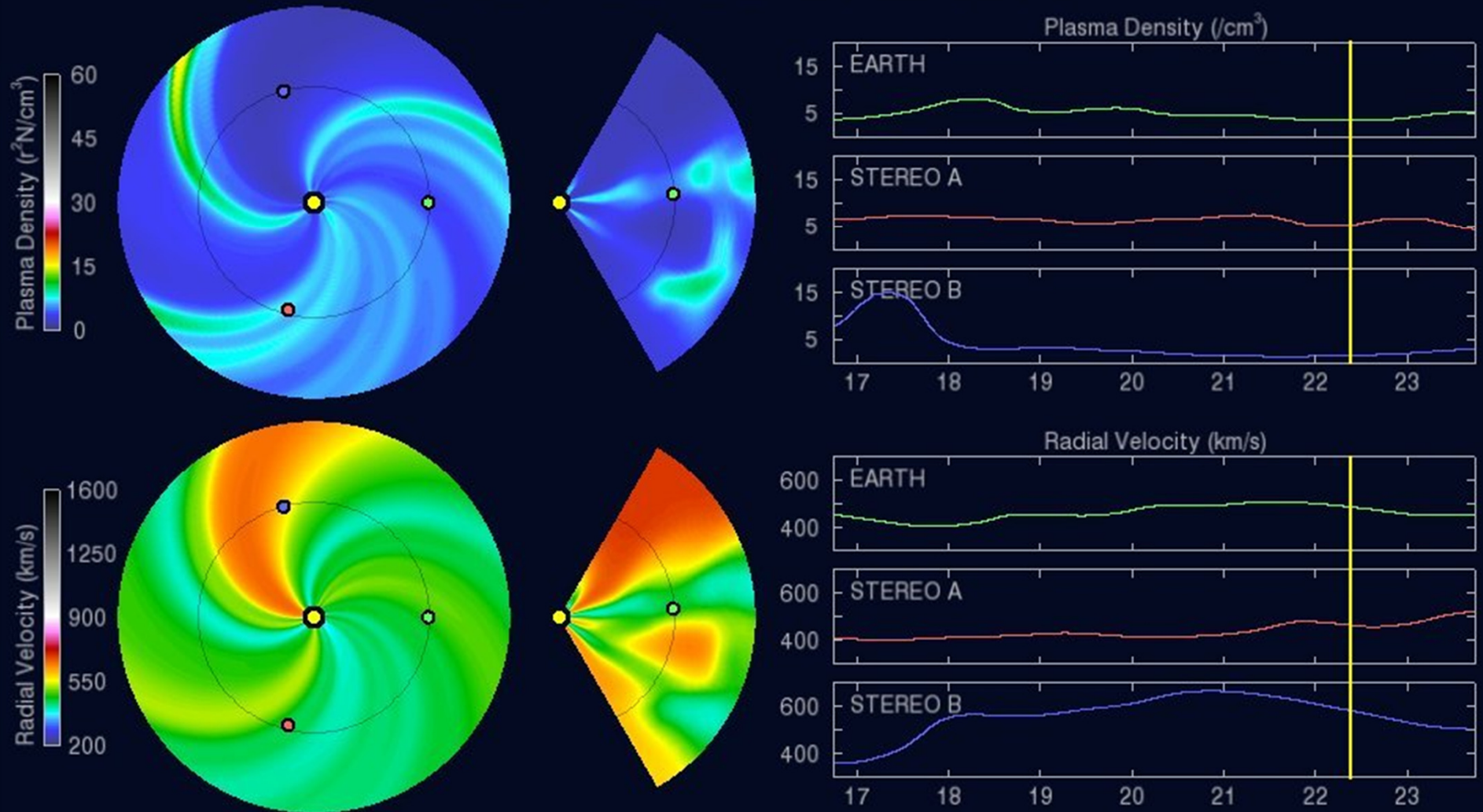
During most of the solar cycle the current sheet is basically a tilted dipole with varying degrees of quadrupole distortion. Near solar maximum the dipole decays leaving a much more complicated structure.

The IMF is a weak field, varying in strength near the Earth from 1 to 37 nT (1 nT =  $10^{-5}$ G), with an average value of 6 nT.

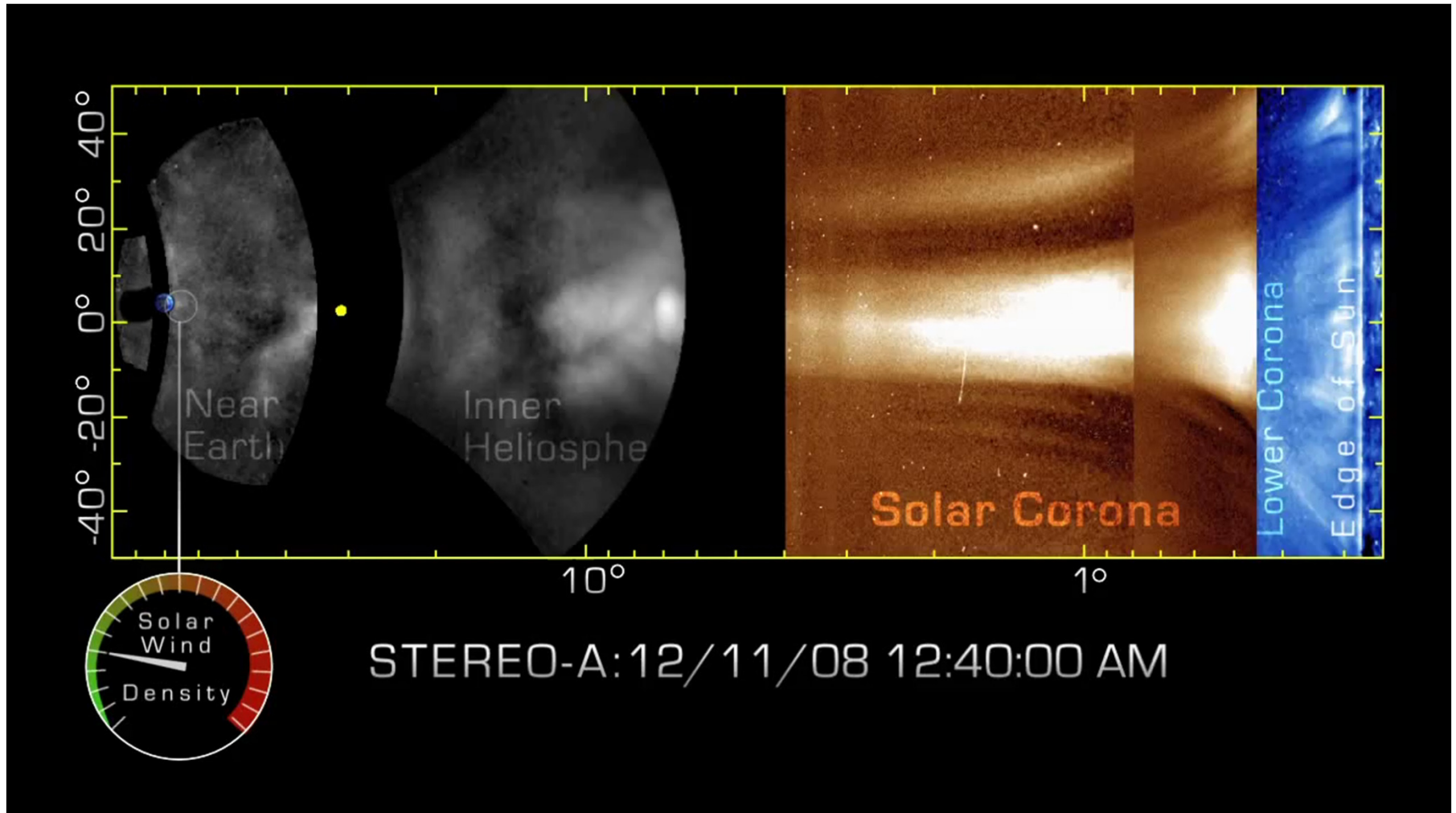
# WSA-ENLIL Solar Wind Prediction Model (MHD)

<http://www.swpc.noaa.gov/products/wsa-enlil-solar-wind-prediction>

2018-11-22 09:00:00



## STEREO-A tracks a Coronal Mass Ejection from the Sun to Earth.



When the CME first left the sun, it was cavernous, with walls of magnetism encircling a cloud of low-density gas. As the CME crossed the Sun-Earth divide, however, its shape changed. The CME "snow-plowed" through the solar wind, scooping up material to form a towering wall of plasma. (DeForest, 2011)

NASA's Mars Atmosphere and Volatile Evolution (MAVEN) mission determined the rate at which the Martian atmosphere currently is losing gas to space via stripping by the solar wind. The findings reveal that the erosion of Mars' atmosphere increases significantly during solar storms. (NASA Press-release, Nov.5, 2015)

